Atmos. Chem. Phys., 16, 13035–13047, 2016
www.atmos-chem-phys.net/16/13035/2016/
doi:10.5194/acp-16-13035-2016

Atmospheric Chemistry and Physics Open Access EGU

The effect of viscosity and diffusion on the HO_2 uptake by sucrose and secondary organic aerosol particles

Pascale S. J. Lakey[1,2], Thomas Berkemeier[2], Manuel Krapf[3], Josef Dommen[3], Sarah S. Steimer[3], Lisa K. Whalley[1,4], Trevor Ingham[1,4], Maria T. Baeza-Romero[5], Ulrich Pöschl[2], Manabu Shiraiwa[2,6], Markus Ammann[3], and Dwayne E. Heard[1,4]

[1]School of Chemistry, University of Leeds, Woodhouse Lane, Leeds, LS2 9JT, UK
[2]Multiphase Chemistry Department, Max Planck Institute for Chemistry, Hahn-Meitner-Weg 1, 55128 Mainz, Germany
[3]Paul Scherrer Institute, Villigen, Switzerland
[4]National Centre for Atmospheric Chemistry, University of Leeds, Woodhouse Lane, Leeds, LS2 9JT, UK
[5]Escuela de Ingeniería Industrial de Toledo, Universidad de Castilla la Mancha, Avenida Carlos III s/n Real Fábrica de Armas, 45071 Toledo, Spain
[6]Department of Chemistry, University of California, Irvine, CA 92617, USA

Correspondence to: Dwayne E. Heard (d.e.heard@leeds.ac.uk)

Received: 1 April 2016 – Published in Atmos. Chem. Phys. Discuss.: 26 April 2016
Revised: 31 August 2016 – Accepted: 19 September 2016 – Published: 21 October 2016

Abstract. We report the first measurements of HO_2 uptake coefficients, γ, for secondary organic aerosol (SOA) particles and for the well-studied model compound sucrose which we doped with copper(II). Above 65 % relative humidity (RH), γ for copper(II)-doped sucrose aerosol particles equalled the surface mass accommodation coefficient $\alpha = 0.22 \pm 0.06$, but it decreased to $\gamma = 0.012 \pm 0.007$ upon decreasing the RH to 17 %. The trend of γ with RH can be explained by an increase in aerosol viscosity and the contribution of a surface reaction, as demonstrated using the kinetic multilayer model of aerosol surface and bulk chemistry (KM-SUB). At high RH the total uptake was driven by reaction in the near-surface bulk and limited by mass accommodation, whilst at low RH it was limited by surface reaction. SOA from two different precursors, α-pinene and 1,3,5-trimethylbenzene (TMB), was investigated, yielding low uptake coefficients of $\gamma < 0.001$ and $\gamma = 0.004 \pm 0.002$, respectively. It is postulated that the larger values measured for TMB-derived SOA compared to α-pinene-derived SOA are either due to differing viscosity, a different liquid water content of the aerosol particles, or an $HO_2 + RO_2$ reaction occurring within the aerosol particles.

1 Introduction

OH and HO_2 radicals play a vital role in atmospheric chemistry by controlling the oxidative capacity of the troposphere, with HO_2 acting as a short-lived reservoir for OH. Oxidation by the OH radical determines the lifetime and concentrations of many trace gases within the troposphere such as NO_x (NO and NO_2), CH_4, and volatile organic compounds (VOCs). The reaction of HO_2 with NO also constitutes an important source of ozone, which is damaging to plants, a respiratory irritant, and a greenhouse gas (Pöschl and Shiraiwa, 2015; Fowler et al., 2009). It is therefore important to have a thorough understanding of the reactions and processes that affect HO_x concentrations. However, during field campaigns HO_2 concentrations have sometimes been measured as being lower than the concentrations predicted by constrained box models implying a missing HO_2 sink, which has often been attributed to HO_2 uptake by aerosol particles (e.g. Kanaya et al., 2007; Mao et al., 2010; Whalley et al., 2010).

SOA is generated from low-volatility products formed by the oxidation of VOCs, and it accounts for a large fraction of the organic matter in the troposphere. For example, in urban areas it can account for up to 90 % of the organic particulate mass (Kanakidou et al., 2005; Lim and Turpin, 2002). Lakey et al. (2015a) previously measured the HO_2

uptake coefficient onto single component organic aerosol particles as ranging from $\gamma < 0.004$ to $\gamma = 0.008 \pm 0.004$ unless elevated transition metal ions that catalyse the destruction of HO_2 were present within the aerosol. Taketani et al. (2013) and Taketani and Kanaya (2010) also measured the HO_2 uptake coefficient onto dicarboxylic acids ($\gamma = 0.02 \pm 0.01$ to $\gamma = 0.18 \pm 0.07$) and levoglucosan ($\gamma < 0.01$ to $\gamma = 0.13 \pm 0.03$) over a range of humidities. However, there are currently no measurements of the HO_2 uptake coefficient onto SOA published in the literature.

Using the kinetic multilayer model of aerosol surface and bulk chemistry (KM-SUB), Shiraiwa et al. (2011b) have shown that the bulk diffusion of a species within an aerosol matrix can have a large impact on a measured uptake coefficient. Diffusion coefficients of a particular species within a particle are related to the viscosity of that particle with larger diffusion coefficients in less viscous particles. Traditionally, the relationship between viscosity and diffusion coefficients is given by the Stokes–Einstein equation, although this relation was found to break down for concentrated solutions and solutions near their glass transition temperature or humidity (Champion et al., 1997; Power et al., 2013). Zhou et al. (2013) have also shown that the rate of heterogeneous reaction of particle-borne benzo[a]pyrene (BaP) with ozone within SOA particles was strongly dependent upon the bulk diffusivity of the SOA. Along the same lines, Steimer et al. (2014, 2015) demonstrated a clear link between the ozonolysis rates of shikimic acid and the changing diffusivity in the transition between liquid and glassy states. Previous measurements of both N_2O_5 uptake coefficients and HO_2 uptake coefficients onto humic acid aerosol particles and N_2O_5 uptake coefficients onto malonic acid and citric acid aerosol particles have shown much lower uptake coefficients at low relative humidities compared to higher humidities (Badger et al., 2006; Thornton et al., 2003; Lakey et al., 2015a; Gržinić et al., 2015). However, viscosity effects have not been investigated systematically for HO_2 uptake, and the first aim of this paper was to investigate whether a change in aerosol viscosity, exemplified using the well-studied model compound sucrose (Berkemeier et al., 2014; Price et al., 2014; Zobrist et al., 2011), could impact the HO_2 uptake coefficient. The second aim of this study was to measure the HO_2 uptake coefficient onto two different types of SOA representative of biogenic and anthropogenic SOA. α-Pinene is the major terpene that forms biogenic SOA, while 1,3,5- trimethylbenzene (TMB) is representative of alkyl benzenes, which are the most abundant aromatic hydrocarbons and form anthropogenic SOA (Calvert et al., 2002; Qi et al., 2012). SOA is known to be highly viscous, with viscosities of 10^3–10^6 Pa s at 50 % RH (Renbaum-Wolff et al., 2013).

2 Experimental setup

The general experimental setup for the Leeds aerosol flow tube and the data analysis methodology to determine values of γ have previously been discussed in detail by George et al. (2013). This is the same experimental setup and data analysis methodology that was used for the copper(II)-doped sucrose experiments, which were also performed at the University of Leeds. Therefore, only a brief description of the setup is included below, with the emphasis being on changes made to the apparatus for the SOA experiments undertaken at the Paul Scherrer Institute (PSI), for which a schematic is shown in Fig. 1. For all experiments the HO_2 radical was released at the end of an injector which was moved backwards and forwards along an aerosol flow tube. The flow from the injector was 1.32 ± 0.05 slpm. For the copper-doped sucrose experiments, the humid aerosol flow was 1.0 ± 0.1 slpm and was mixed with a much drier flow (with the humidity of this flow being controlled by mixing a flow from a water bubbler with a dry flow in different ratios) of 3.0 ± 0.3 slpm within a conditioning flow tube for approximately 10 s before entering the aerosol flow tube. Nitrogen was used for all of these flows. For the SOA experiments the flow from the smog chamber or potential aerosol mass (PAM) chamber at PSI was 4.0 ± 0.3 slpm. Decays of the HO_2 radical along an aerosol flow tube were measured using a fluorescence assay by gas expansion (FAGE) detector in both the absence and presence of different concentrations of aerosol particles. All experiments were performed at room temperature (293 ± 2 K).

The HO_2 radical was formed via Reactions (R1)–(R2), by passing a humidified flow over a mercury pen-ray lamp (L.O.T. Oriel, model 6035) in the presence of trace amounts (20–30 ppm) of oxygen in the nitrogen flow.

$$H_2O + h\nu \rightarrow OH + H \quad \text{(R1)}$$

$$H + O_2 + M \rightarrow HO_2 + M \quad \text{(R2)}$$

Data acquisition was only started once HO_2 concentrations within the flow tube were stable, which occurred within 1 min of switching on the mercury lamp. The HO_2 radicals entered the FAGE cell through a 0.7 mm diameter pinhole and were then converted to OH by reacting with added NO. The FAGE cell was either kept at a pressure of ~ 0.85 or ~ 1.5 Torr using a combination of a rotary pump (Edwards, model E1M80) and a roots blower (EH1200). The OH radicals were detected by laser-induced fluorescence at 308 nm (Heard and Pilling, 2003; Stone et al., 2012). Initial HO_2 concentrations (obtained by calibration) exiting the injector were measured as $\sim 1 \times 10^9$ molecule cm^{-3} for all experiments (following mixing and dilution with the main flow), and the concentration was then measured as a function of distance along the flow tube.

For the experiments using copper-doped sucrose aerosol particles, 3.42 g of sucrose (Fisher, > 99 %) and 0.125 g of

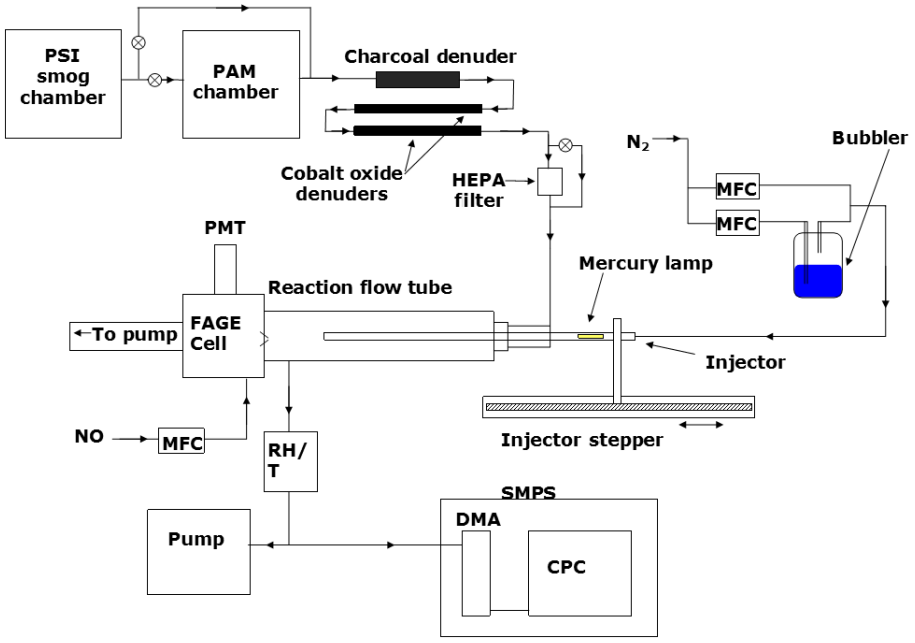

Figure 1. A schematic of the experimental setup used to measure HO_2 uptake coefficients onto SOA aerosol particles. Key: PAM – potential aerosol mass; PMT – photomultiplier tube; FAGE – fluorescence assay by gas expansion; MFC – mass flow controller; RH/T – relative humidity and temperature probe; SMPS – scanning mobility particle sizer; DMA – differential mobility analyser; CPC – condensation particle counter; HEPA – high-efficiency particulate arresting.

copper(II) sulfate pentahydrate were dissolved in 500 mL of milliQ water. These solutions were then placed in an atomizer (TSI, 3076) in order to form aerosol particles. The aerosol particles passed through a neutralizer (Grimm 5522) and an impactor before entering the conditioning flow tube. The size distribution of the aerosol particles was then measured at the end of the reaction flow tube using a scanning mobility particle sizer (SMPS, TSI, 3080).

The experimental setup used to measure previous HO_2 uptake coefficients (George et al., 2013; Matthews et al., 2014; Lakey et al., 2015a, b) was transported from the University of Leeds, UK, to the Paul Scherrer Institute, Switzerland, where it was connected to the Paul Scherrer Institute (PSI) smog chamber and, for some of the experiments, also to a PAM chamber (see Fig. 1). The PSI smog chamber has a volume of 27 m^3, it is made from 125 µm Teflon fluorocarbon film, and has been described elsewhere (Paulsen et al., 2005). To initiate photochemical reactions four 4 kW xenon arc lamps (light spectrum > 280 nm, OSRAM) and 80 black lights (100 W tubes, light spectrum between 320 and 400 nm, Cleo Performance) were used. For most experiments the chamber was first humidified to 50 % relative humidity, but for two experiments this was increased to 80 %, after which the precursor gases were added. The concept, design and operation of a PAM chamber has also previously been described (Kang et al., 2007). The PAM chamber at PSI is a flow tube of 0.46 m in length and 0.22 m internal diameter. Two low-pressure Hg lamps mainly emitting at 185 and 254 nm produce ozone in the chamber. Water vapour was photolysed by the 185 nm radiation to produce OH and HO_2, and the radiation also photolysed O_2 to produce O_3, whereas the 254 nm light could also photolyse O_3 to produce OH following the reaction of $O(^1D)$ with water vapour. Upper-limit OH production rates are in the range of $1–2 \times 10^{12}$ molecule cm^{-3} s^{-1} (Bruns et al., 2015). The composition and oxidation state of SOA formed within PAM chambers has previously been shown to be similar to SOA generated within environmental chambers (Bruns et al., 2015; Lambe et al., 2011a) and SOA in the atmosphere (Ortega et al., 2016).

Four different types of experiments were performed:

i. α-pinene ozonolysis in the PSI smog chamber (600 ppb α-pinene, 280 ppb ozone: ozone was added first to the chamber; after injection of α-pinene, particle nucleation and growth rapidly occurred);

ii. OH-initiated α-pinene photochemistry in the smog chamber (500 ppb α-pinene, 350 ppb NO_2: xenon and black lights were used to initiate photochemical reactions);

iii. OH-initiated α-pinene photochemistry in the PAM chamber (500 ppb α-pinene was filled into the large smog chamber at 50 or 80 % RH to supply a constant concentration of α-pinene to the PAM chamber; all SOA was formed within the PAM chamber);

iv. OH-initiated TMB photochemistry in the PAM chamber (2 ppm TMB was filled into the large smog chamber at 50 % RH to supply a constant concentration of TMB to the PAM chamber; all SOA was formed within the PAM chamber).

These precursor concentrations were chosen in order to obtain a large enough aerosol surface area in the flow tube to be able to measure an HO_2 uptake coefficient. Experiments were performed only once the aerosol surface area within the aerosol flow tube exceeded 5×10^{-5} cm^2 cm^{-3} and in the case of the smog chamber experiments once a maximum aerosol concentration had been reached (as summarized in the Results section). Prior to entering the flow tube, the aerosol flow from the smog or PAM chamber (4.0 slpm) was passed through either two or three cobalt oxide denuders in series (each 40 cm long, 0.8 cm inner diameter quartz tubes coated with cobalt oxide prepared by thermal decomposition of a saturated $Co(NO_3)_2$ solution applied to its inner walls at 700 °C as described in Ammann, 2001), which in turn were in series with a charcoal denuder (length: 16.4 cm; diameter: 0.9 cm; 69 quadratic channels) in order to remove NO_x species, RO_2, VOCs, and ozone that had been present in the chamber. These denuders have previously been shown to be extremely efficient at removing gas-phase NO_x and VOCs (Arens et al., 2001). It should be noted that the flows were drawn through the aerosol flow tube using a pump instead of the normal procedure whereby the flows are pushed through the experimental setup using mass flow controllers. The pumping setup led to slightly reduced pressures (904–987 mbar) in the aerosol flow tube, and so careful checks were performed to ensure that the flow tube was vacuum tight. The aerosol size distribution from which the surface area exiting the flow tube was calculated was measured using an SMPS, which consisted of a neutralizer (Kr-85), a differential mobility analyser (DMA; length 93.5 cm, inner radius 0.937 cm, and outer radius 1.961 cm), and a condensation particle counter (CPC; TSI, model 3022). A typical surface-weighted aerosol size distribution for the α-pinene-derived aerosol particles is shown in Fig. 2. Note that an impactor was not used in the experimental setup for the SOA measurements as this restricted the flow that could be pumped through the flow tube and was also found to be unnecessary as the aerosol size distribution from the chambers fell entirely within the range of aerosol sizes that the SMPS could measure.

In order to check that the experimental setup used at PSI produced consistent results with those previously performed at the University of Leeds, an experiment was performed with ammonium sulfate aerosol particles. The ammonium sulfate aerosol particles were formed using an atomizer rather than in a chamber but were then passed through the same setup (including the denuders) as the SOA was passed through. The experiment was performed at a flow tube pressure of 915 mbar, due to the flows being pumped through the setup (compared to pressures of 904–987 mbar for the SOA experiments), and an HO_2 uptake coefficient of 0.004 ± 0.002 was measured at 60 % RH, which is in agreement with previous experiments by George et al. (2013), which were performed at atmospheric pressure (∼ 970–1040 mbar).

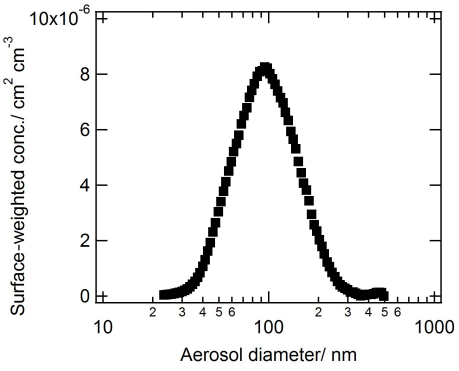

Figure 2. An example of the size distribution for α-pinene-derived aerosol particles formed in the PAM chamber at a relative humidity of ∼ 50 %.

3 Data analysis

Experiments were performed by moving the HO_2 injector backwards and forwards along the flow tube either in the presence of or in the absence of aerosol particles and recording the FAGE signal from HO_2 radicals. The background signal in the absence of HO_2 (mercury lamp in the injector switched off), but with the NO entering the FAGE cell, was recorded and was subtracted from the signal during experiments. For α-pinene experiments this background signal was small and similar to previous experiments using dust as well as organic and inorganic salt aerosol particles (George et al., 2013; Lakey et al., 2015a, b; Matthews et al., 2014). However, for the TMB experiments this background signal varied from about half to two thirds of the signal from HO_2 with the mercury lamp in the injector switched on. The background signal disappeared when the NO added to the FAGE cell was switched off, showing that it was not due to OH. The background signal within experiments did not change when aerosol particles were present compared to when they were completely filtered out (see Fig. 1). Although the denuders are efficient at removing gas-phase species (Arens et al., 2001), it can be hypothesized that the signal was due to the formation of HO_2 and RO_2 radicals generated by a small fraction of ozone, precursors, and oxidation products passing through the denuders for the TMB experiments. RO_2 species would have been observed as an HO_2 interference by the FAGE detection method. FAGE interferences have previously been observed for alkene, aromatic, and > C3 alkane-derived RO_2 (Fuchs et al., 2011; Whalley et al., 2013). A

box model was run, utilizing chemistry within the Master Chemical Mechanism (MCM 3.2), which is detailed further in Whalley et al. (2013), and constrained to the experimental concentrations, and it showed that the expected interference from TMB RO_2 and α-pinene RO_2 would have been equivalent to $0.59 \times [HO_2]$ and $0.44 \times [HO_2]$, respectively, at an NO flow of 50 mL min^{-1} into the FAGE cell, a FAGE pressure of 1.5 Torr, and a flow through the FAGE pinhole of 4.2 slpm. However, for α-pinene experiments the background signal did not change between the NO being switched on and off with the mercury lamp switched off in the injector, indicating the absence of interferences in the FAGE cell for these experiments. We hypothesize that the lack of interference for the α-pinene experiments suggests that the denuders were more efficient at removing the gas-phase precursors and oxidation products from the chamber and that only negligible concentrations of RO_2 species were present in the flow tube. Nevertheless, since for the TMB experiments a significant background signal was observed, that signal was measured regularly throughout the experiment and used to correct the measurement data.

HO_2 decays along the flow tube in the presence and absence of aerosol particles were measured between ~ 10 and 18 s flow time after the point of injection to ensure thorough mixing. A previous calculation showed that the flows should be fully mixed by ~ 7 s (George et al., 2013). An example of the HO_2 decays in the presence and absence of aerosol particles for a TMB experiment is shown in Fig. 3, plotted as the natural logarithm of the HO_2 signal (proportional to concentration) against reaction time according to:

$$\ln \frac{[HO_2]_t}{[HO_2]_0} = -k_{obs} t. \quad (1)$$

There is clear uptake of HO_2 observed by the SOA derived from TMB. The pseudo first-order rate coefficients (k_{obs}) were then corrected for wall losses and non-plug flow conditions using the methodology described by Brown (1978). The average correction was 22 %. These corrected rate coefficients (k') were related to the HO_2 uptake coefficient (γ_{obs}) by the following equation:

$$k' = \frac{\gamma_{obs} \omega_{HO_2} S}{4}, \quad (2)$$

where ω_{HO_2} is the molecular thermal speed of HO_2 and S is the total aerosol surface area. Examples of k' as a function of the aerosol surface area are shown in Fig. 4. The HO_2 uptake coefficients were then corrected for gas-phase diffusion limitations using the methodology described by Fuchs and Sutugin (1970), although this correction changed the uptake coefficient by less than 1 % for all experiments.

4 Model description

The kinetic multilayer model of aerosol surface and bulk chemistry (KM-SUB) has been described in detail by Shiraiwa et al. (2010). It is a multilayer model comprising a gas phase, a near-surface gas phase, a sorption layer, a near-surface bulk layer, and a number of bulk layers arranged in spherical geometry. Processes that can occur within the model include gas-phase diffusion, adsorption and desorption, bulk diffusion, and chemical reactions in the gas phase at the surface and in the bulk. In contrast to traditional resistor models, the KM-SUB model enables efficient treatment of complex chemical mechanisms. Input parameters to the model are summarized in Table 1, whilst the reactions that were included are shown below:

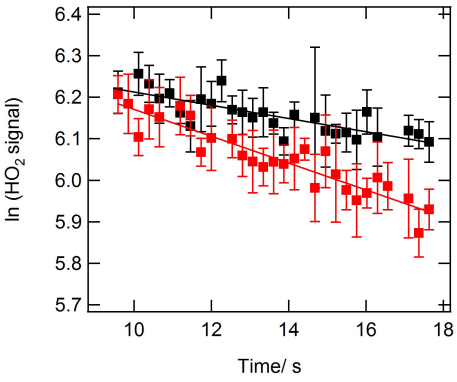

Figure 3. Examples of the HO_2 wall loss without any aerosol particles along the flow tube (black squares) and the HO_2 loss with an aerosol surface area of 2.2×10^{-4} cm^2 cm^{-3} for TMB-derived aerosol particles at an initial HO_2 concentration of $\sim 1 \times 10^9$ molecule cm^{-3} (red squares) and for RH = 50 %. The error bars represent 1 standard deviation in the measured HO_2 signal for a measurement time per point of 3 s.

$$HO_{2(g)} + HO_{2(g)} \rightarrow H_2O_{2(g)} + O_{2(g)} \quad k_{GP} \quad (R3)$$

$$HO_{2(aq)} \rightleftharpoons H^+_{(aq)} + O^-_{2(aq)} \quad K_{eq} \quad (R4)$$

$$HO_{2(aq)} + HO_{2(aq)} \rightarrow H_2O_{2(aq)} + O_{2(aq)} \quad k_{BR,1} \quad (R5)$$

$$HO_{2(aq)} + O^-_{2(aq)} + H_2O_{(l)} \rightarrow H_2O_{2(aq)} + O_{2(aq)} + OH(aq)^- \quad k_{BR,2} \quad (R6)$$

$$Cu^{2+}_{(aq)} + HO_{2(aq)} \rightarrow O_{2(aq)} + Cu^+_{(aq)} + H^+_{(aq)} \quad k_{BR,3} \quad (R7)$$

$$Cu^{2+}_{(aq)} + O^-_{2(aq)} \rightarrow O_{2(aq)} + Cu^+_{(aq)} \quad k_{BR,4} \quad (R8)$$

$$Cu^+_{(aq)} + HO_{2(aq)} + H_2O_{(l)} \rightarrow H_2O_{2(aq)} + Cu^{2+}_{(aq)} + OH^-_{(aq)} \quad k_{BR,5} \quad (R9)$$

$$Cu^+_{(aq)} + O^-_{2(aq)} + 2H_2O_{(l)} \rightarrow H_2O_{2(aq)} + Cu^{2+}_{(aq)} + 2OH^-_{(aq)} \quad k_{BR,6}. \quad (R10)$$

The bulk layer number was set to 100, corresponding to a bulk layer thickness of 0.5 nm, which is only slightly larger

Table 1. The parameters used in the KM-SUB HO_2 uptake model over all relative humidities.

Parameter	Description	Value at 293 K	Reference
$k_{BR,1}$	Rate coefficient, R5	1.3×10^{-15} cm^3 s^{-1}	Thornton et al. (2008)
$k_{BR,2}$	Rate coefficient, R6	1.5×10^{-13} cm^3 s^{-1}	Thornton et al. (2008)
$k_{BR,3}$	Rate coefficient, R7	1.7×10^{-13} cm^3 s^{-1}	Jacob (2000)
$k_{BR,4}$	Rate coefficient, R8	1.3×10^{-11} cm^3 s^{-1}	Jacob (2000)
$k_{BR,5}$	Rate coefficient, R9	2.5×10^{-12} cm^3 s^{-1}	Jacob (2000)
$k_{BR,6}$	Rate coefficient, R10	1.6×10^{-11} cm^3 s^{-1}	Jacob (2000)
k_{GP}	Rate coefficient, R3	3×10^{-12} cm^3 s^{-1}	Sander et al. (2003)
K_{eq}	Equilibrium constant, R4	2.1×10^{-5} M	Thornton et al. (2008)
H_{cp,HO_2}	HO_2 Henry's law constant	5600 M atm^{-1}	Thornton et al. (2008)
τ_d	HO_2 desorption lifetime	1.5×10^{-3} s	Shiraiwa et al. (2010)
$\alpha_{s,0}$	HO_2 surface accommodation at time 0	0.22	
D_{g,HO_2}	HO_2 gas-phase diffusion rate coefficient	0.25 cm^{-2} s^{-1}	Thornton et al. (2008)
[Cu(II)]	Copper concentration (used when modelling copper-doped sucrose aerosol particles)	5×10^{19} cm^{-3}	
T	Temperature	293 K	

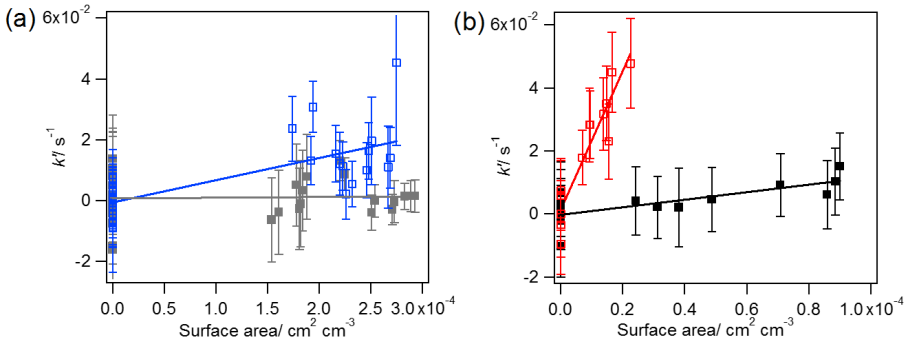

Figure 4. The pseudo first-order rate coefficients with the wall losses subtracted as a function of aerosol surface area for **(a)** α-pinene-derived aerosol particles (grey) and TMB-derived aerosol particles (blue) at 50 % RH and a pressure of 904–929 mbar and **(b)** copper-doped sucrose aerosol particles at 17 % RH (black) and 71 % RH (red) at atmospheric pressure. Experiments were performed at 293 ± 2 K. In **(a)** experiments were performed using the PAM chamber as the source of aerosol particles and represent experiments 5 and 6 in Table 2. Error bars represent the 1 SD (standard deviation) propagated uncertainty for individual determinations of k'. The data points at an aerosol surface area of 0 cm^2 cm^{-3} (no aerosol particles present) are repeats of the wall loss decays taken throughout the experiment and are within error of each other.

than the diameter of HO_2 (0.4 nm) and implies that HO_2 only needs to travel approximately the distance of its own diameter to go from being an adsorbed radical on the surface of the aerosol particle to a dissolved aqueous radical. The same short distance must be overcome by HO_2 to move between bulk layers, which is important for the convergence of the numerical model, especially when the chemical reactions within the aerosol particles are very fast compared to the diffusion timescales, leading to steep concentration gradients within the particle. Reducing the bulk layer thickness further did not significantly impact the calculated uptake coefficients.

During experiments the average radius was observed to change by less than 10 % over the range of humidities, and therefore an assumption was made within the model that the average aerosol radius remained constant over the range of relative humidities. For the diffusion coefficient of HO_2 within aerosol particles, we used the measured diffusion coefficients of H_2O within sucrose solutions, which we then corrected using the Stokes–Einstein equation to take into account the larger radius of HO_2 radicals compared to H_2O molecules (Price et al., 2014; Zobrist et al., 2011). The correction resulted in a factor of 1.22 decrease in the diffusion coefficients of HO_2 compared to the diffusion coefficients of H_2O. It should be noted that above a viscosity of 10 Pa s the Stokes–Einstein relationship starts to fail and that the effect of increasing molecular size may become much stronger (Power et al., 2013). Price et al. (2014) estimated diffusion coefficients of H_2O by using Raman spectroscopy to observe D_2O diffusion in high-viscosity sucrose solutions, whilst Zo-

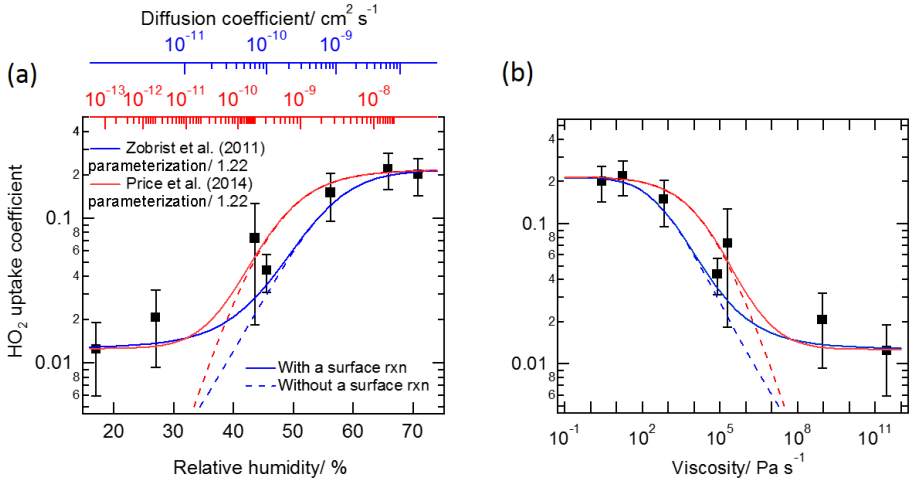

Figure 5. The HO_2 uptake coefficient onto copper (II)-doped sucrose aerosol particles as a function of **(a)** relative humidity and **(b)** aerosol particle viscosity. The lines represent the expected HO_2 uptake coefficient calculated using the KM-SUB model using the Price et al. (2014) (red) and Zobrist et al. (2011) (blue) diffusion parameterizations (see model description section) with (solid) and without (dashed) the inclusion of a surface reaction (Reaction R11). The viscosity within sucrose aerosol particles is based upon the data and fitting shown in Power et al. (2013) and Marshall et al. (2016), whilst the red and blue axes in **(a)** are the Price et al. (2014) and Zobrist et al. (2011) diffusion parameterizations, respectively. The error bars represent 2 standard deviations of the propagated error in the gradient of the k' against aerosol surface area graphs.

brist et al. (2011) used optical techniques to observe changes in the size of sucrose particles when exposed to different relative humidities.

Sensitivity tests showed that the diffusion rate coefficients of O_2^-, Cu^+, and Cu^{2+} did not influence calculation results. The reaction rate coefficients involving copper ($k_{BR,3} - k_{BR,6}$) are so large that O_2^- is produced in situ and consumed locally. The catalytic nature of these reactions causes Cu^+ and Cu^{2+} to rapidly interconvert meaning that they remain available at high concentrations in the upper layers of the aerosol particle. Similarly, as sucrose does not react with any species within the model, its diffusion within the model is unimportant to the outputted HO_2 uptake coefficient.

5 Results and discussion

5.1 HO_2 uptake by copper-doped sucrose aerosol particles

The results of the HO_2 uptake coefficient measurements onto copper-doped sucrose aerosol particles as a function of relative humidity (RH) are shown in Fig. 5. The results show a large dependence upon relative humidity, with the HO_2 uptake coefficient increasing from 0.012 ± 0.007 at 17 ± 2 % RH to 0.22 ± 0.06 at relative humidities above 65 %. The latter value is likely equal to the surface accommodation coefficient and is consistent with many previous studies (Takahama and Russell, 2011; George et al., 2013; Lakey et al., 2015b). At lower humidities, the diffusion coefficients decrease, which leads to slower transport of HO_2 within the bulk and therefore to a slower overall rate of HO_2 destruction (Reactions 7–10). The HO_2 reacto-diffusive length (Hanson et al., 1994; Schwartz and Freiberg, 1981) varied from between $\sim$ 4 and 7 nm at the highest relative humidity that was used (71 % RH) down to $\sim$ 0.006–0.05 nm at the lowest relative humidity (17 % RH). The range of values for the reacto-diffusive length at a given RH is due to the difference between the parameterizations of the diffusion coefficient in Price et al. (2014) and Zobrist et al. (2011). These reacto-diffusive lengths indicate that at all relative humidities HO_2 radicals will be limited to the outermost molecular layers of the particle before reacting away, which is in agreement with the model. Note that it was shown previously that the uptake of gas-phase species generally increases with increasing reacto-diffusive length, which is consistent with our HO_2 uptake coefficient measurements (Slade and Knopf, 2014; Davies and Wilson, 2015; Houle et al., 2015). The red and blue lines in Fig. 5 show the predicted HO_2 uptake coefficients using the KM-SUB model when using two different parameterizations for HO_2 diffusion coefficients as a function of RH (see the model description). There is good agreement between the model and the measurements, suggesting that the change in HO_2 uptake over the range of humidities is indeed due to a change in the HO_2 diffusion coefficient which is in turn due to a change in the viscosity of the aerosol particles. Sensitivity tests showed that an increase in the rate coefficients of Reactions (R7)–(R10) does not affect the HO_2 uptake coefficient. A decrease of 2 orders of magnitude in the rate coefficients affects the uptake coefficient marginally by

reducing it by less than 10 % in the 40–55 % relative humidity range, but it has no impact at the lower or higher relative humidities.

Using the kinetic framework and classification scheme of Berkemeier et al. (2013), Fig. 6 illustrates how the change in relative humidity leads to a change in the kinetic regime of HO_2 uptake. At the highest relative humidities the uptake is limited by surface accommodation. At intermediate relative humidities with $\gamma < \alpha_{s,0}$, the uptake is limited by surface-to-bulk transport, which is related to both solubility (Henry's law coefficient) and diffusivity (diffusion coefficient) in the kinetic model. Under humid conditions, the uptake is driven by chemical reaction in the near-surface bulk and effectively limited by mass accommodation, which includes both surface accommodation and surface-to-bulk transport (Behr et al., 2009; Berkemeier et al., 2013). At low relative humidities the HO_2 uptake coefficient was limited by chemical reaction at the surface as discussed below (Berkemeier et al., 2013).

Although the viscosity changes by more than 8 orders of magnitude and the diffusion coefficients change by 5–7 orders of magnitude over the investigated range of relative humidity, the measured HO_2 uptake coefficients change by only ~ 1 order of magnitude. This can be explained to some extent by the uptake coefficient being proportional to the square root of the diffusion coefficient when the uptake is controlled by reaction and diffusion of HO_2 in the bulk (Davidovits et al., 2006; Berkemeier et al., 2013). If this were the only mechanism involved, however, one would still expect a change in the uptake coefficient by 2.5–3.5 orders of magnitude. The most plausible explanation for the relatively high HO_2 uptake coefficients observed at low relative humidities is a surface reaction of HO_2. For example, at 17 % RH and without a surface reaction, γ values as low as $\sim 5 \times 10^{-4}$ and $\sim 3 \times 10^{-5}$ would be expected using the Zobrist et al. (2011) and Price et al. (2014) parameterizations, respectively. However, by including the following self-reaction of HO_2 at the surface of the sucrose particles, much better agreement with the observed values of around $\sim 10^{-2}$ could be obtained (Fig. 5):

$$HO_2 + HO_2 \xrightarrow{Cu^{2+/+}} H_2O_2 + O_2$$
$$k_{Surf} = 1 \times 10^{-8}\ cm^2\ s^{-1}. \quad \text{(R11)}$$

Although the true mechanism for reaction at the surface remains unclear, the large rate coefficient for this reaction suggests that copper could potentially be catalysing the destruction of HO_2 at the surface of the sucrose particles, which is consistent with the higher HO_2 uptake coefficients measured on solid aerosol particles containing transition metals compared to solid aerosol particles containing no transition metal ions (Matthews et al., 2014; Lakey et al., 2015a; Bedjanian et al., 2013; George et al., 2013). Note however that for a relevant surface reaction in kinetic flux models, it is necessary to use an effective desorption lifetime, τ_d, in the millisecond to second time range (Berkemeier et al., 2016; Shiraiwa et al., 2010). This is many orders of magnitude longer than would be expected due to pure physisorption as estimated by molecular dynamic simulations (Vieceli et al., 2005), indicating that the adsorption process should involve chemisorption or formation of long-lived intermediates that would have the potential to extend these effective desorption lifetimes (Shiraiwa et al., 2011a; Berkemeier et al., 2016). Surface reactions in viscous aqueous organics are consistent with previous work by Gržinić et al. (2015), Steimer et al. (2015), and Berkemeier et al. (2016) for the uptake of N_2O_5 to citric acid and the uptake of O_3 to shikimic acid over a range of relative humidities. A second potential reason for the discrepancy at low humidities could be an incomplete equilibration of the aerosol particles with respect to RH, as they had only been mixed with the conditioning flow for ~ 10 s before entering the reaction flow tube. Bones et al. (2012) inferred from measurements on larger particles that for 100 nm diameter sucrose aerosol particles, the equilibration time would be more than 10 s when the viscosity increased above $\sim 10^5$ Pa s, which would occur at ~ 43 % RH (Power et al., 2013). The actual diffusion coefficients would thus be higher than assumed in calculations which assume fully equilibrated particles. However, the near-surface bulk of the aerosol particles, where the reactions occur, would be much better equilibrated with respect to RH than the inner core of the aerosol particles (Berkemeier et al., 2014). This means that the lack of aerosol equilibration with respect to RH is likely to have a negligible impact upon the HO_2 uptake coefficient.

It should also be noted that the KM-SUB modelling results were very sensitive to the initial aerosol pH. For example, at a pH of 4.1 (used in Fig. 5; the reason for this value is discussed below), the HO_2 uptake coefficient as predicted by the KM-SUB model at 50 % RH (using the Zobrist et al., 2011, H_2O diffusion coefficients) was $\gamma = 0.06$ compared to $\gamma = 0.11$ at pH 5 and $\gamma = 0.21$ at pH 7. The reason for this strong dependence upon pH has been discussed previously and is due to the partitioning of HO_2 with its conjugate base O_2^-, as shown by Reaction (R4), affecting the effective Henry's law coefficient and the effective rate coefficients (Thornton et al., 2008). Although it was not possible to measure the actual pH of the aerosol particles, it was possible to estimate the concentration of copper(II) sulfate (which is a weak acid) within the aerosol particles using the known growth factors of sucrose aerosol particles (Lu et al., 2014). The pH of 0.05 and 0.1 M copper(II) sulfate solutions (which were calculated to be the extremes of the possible copper concentrations over the RH range) were then measured using a pH meter (Jenway, 3310) as being in the range of 4.10 ± 0.05. It is expected that the pH would be dominated by the presence of copper sulfate rather than sucrose which has a pH of 7 in water and a very high pKa of 12.6. Therefore, there is confidence that the correct initial aerosol pH was inputted into the model. Hence, while the HO_2 uptake coefficient might depend on further factors such as aerosol pH, a clear dependence on relative humidity and hence particle viscosity could be observed, and

Table 2. Summary of the reactants and conditions that were utilized and the HO_2 uptake coefficients that were measured during the experiments. Experiments 1–4 were performed using the smog chamber, whereas experiments 5–9 utilized the PAM chamber.

Experiment number	Reaction type	Initial precursor concentrations	UV	Relative humidity in the chamber/ %	Pressure in the flow tube/ mbar	Maximum aerosol surface to volume ratio in the flow tube/ $cm^2\ cm^{-3}$	HO_2 uptake coefficient (γ)
1	α-Pinene ozonolysis	[α-Pinene]: 600 ppb [O_3]: 280 ppb	Off	50	987	6.30×10^{-5}	< 0.01
2	α-Pinene ozonolysis	[α-Pinene]: 600 ppb [O_3]: 280 ppb	Off	50	965	1.30×10^{-4}	< 0.004
3	α-Pinene ozonolysis	[α-Pinene]: 200 ppb [O_3]: 310 ppb	Off	80	939	7.10×10^{-5}	< 0.006
4	α-Pinene photochemistry	[α-Pinene]: 500 ppb [NO_2]: 350 ppb	On	50	940	6.30×10^{-5}	< 0.018
5	α-Pinene photochemistry	[α-Pinene]: 500 ppb	On	50	929	2.93×10^{-4}	< 0.001
6	TMB photochemistry	[TMB]: 2 ppm	On	50	923	2.75×10^{-4}	0.004 ± 0.002
7	TMB photochemistry	[TMB]: 2 ppm	On	50	918	2.32×10^{-4}	0.004 ± 0.003
8	α-Pinene photochemistry	[α-Pinene]: 500 ppb	On	50	927	1.88×10^{-4}	< 0.005
9	α-Pinene photochemistry	[α-Pinene]: 1 ppm	On	80	904	3.90×10^{-4}	< 0.001

it remains likely that at low humidity a surface loss process becomes dominant.

5.2 HO_2 uptake by SOA

A summary of all HO_2 uptake experiments performed on SOA is shown in Table 2. On average the HO_2 uptake coefficient was measured as 0.004 ± 0.002 on TMB-derived aerosol particles produced in the PAM chamber, whereas for α-pinene-derived aerosol particles only an upper limit of 0.001 (obtained from the error in the slope of Fig. 4a) could be placed on the HO_2 uptake coefficient at 50 and 80 % RH. It should be noted that for the α-pinene experiments the HO_2 uptake coefficient was non-measurable for both ozonolysis and photochemistry experiments using both the smog chamber and the PAM chamber as sources of the SOA, and therefore only upper limits of individual experiments are reported in Table 2. There was some variability for the upper limits that were measured for individual α-pinene experiments, which is likely to be due to the maximum aerosol surface-to-volume ratio that was obtained in each experiment.

There are several possible reasons for the larger HO_2 uptake coefficients being measured for the TMB-derived aerosol particles compared to the α-pinene-derived aerosol particles. These reasons will be summarized below but include a differing particle viscosity, a different particle liquid water content, or an $HO_2 + RO_2$ reaction occurring within the aerosol particles. Although the viscosity of α-pinene-derived aerosol has been measured as $\sim 10^3$ Pa s at 70 % RH and $> 10^9$ Pa s for RH < 30 %, to our knowledge, there are currently no measurements of the viscosity of TMB-derived aerosol published in the literature (Renbaum-Wolff et al., 2013). By running the KM-SUB model, it can be estimated that the diffusion coefficient of HO_2 within the particles would need to be approximately $1 \times 10^{-10}\ cm^2\ s^{-1}$ for TMB-derived aerosol particles and $< 5 \times 10^{-12}\ cm^2\ s^{-1}$ for α-pinene-derived aerosol particles. This range of values seems to be consistent with the diffusion coefficients estimated by Berkemeier et al. (2014) and Lienhard et al. (2015) for water diffusion in low and medium O : C SOA.

Thornton et al. (2003) previously suggested that for malonic acid aerosol particles, the liquid water content could be

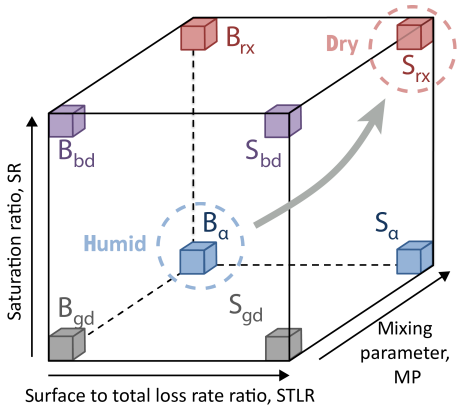

Figure 6. The kinetic cube representing the eight limiting cases for uptake of gases to aerosol particles (Berkemeier et al., 2013). B_{rx}: bulk reaction limited by chemical reaction; B_{bd}: bulk reaction limited by bulk diffusion of the volatile reactant and the condensed reactant; B_{α}: bulk reaction limited by mass accommodation; B_{gd}: bulk reaction limited by gas-phase diffusion; S_{rx}: surface reaction limited by chemical reaction; S_{bd}: surface reaction limited by bulk diffusion of a condensed reactant; S_{α}: surface reaction limited by surface accommodation; S_{gd}: surface reaction limited by gas-phase diffusion. For copper-doped sucrose aerosol particles, the HO_2 uptake coefficient is limited by mass accommodation under humid conditions and by chemical reaction at the surface at low relative humidity.

limiting the aqueous chemistry below 40 % RH. As can be seen by the HO_2 reaction scheme, the rate of Reaction (R6) is dependent upon the liquid water concentration within the aerosol, and therefore the uptake coefficient could be limited by a low aerosol liquid water content. However, there remains some uncertainty as to whether the liquid water content of TMB-derived aerosol particles would be higher than the liquid water content of α-pinene-derived aerosol particles. Duplissy et al. (2011) measured a higher hygroscopicity parameter (κ_{org}) for TMB-derived aerosol particles compared to α-pinene-derived aerosol particles, whereas Lambe et al. (2011b) and Berkemeier et al. (2014) stated the opposite. However, as well as being dependent upon the hygroscopicity parameter, the liquid water content of the aerosol particles would also be dependent upon the O : C ratio in the SOA.

If the viscosity and liquid water content of the α-pinene and TMB-derived aerosol particles are similar, the larger HO_2 uptake coefficients measured for TMB-derived aerosol particles could be due to a higher reactivity of these aerosol particles towards HO_2. This could be the case if the TMB-derived aerosol particles contained reactive radical species such as organic peroxy radicals, RO_2, which partition into the aerosol or are formed within the aerosols by intra-particular reactions (Donahue et al., 2012; Lee et al., 2016). As previously stated in the "Data analysis" section, during α-pinene experiments, no indication of RO_2 being present in the flow tube was observed by FAGE as an HO_2 interference. However, for TMB-derived aerosol particles, a large background signal was observed by FAGE, indicating that reactive radical species were likely to be present within the flow tube. If the reaction of HO_2 with these species at the surface or within the bulk of the aerosol was faster than the equivalent gas-phase reaction, a larger HO_2 uptake coefficient would be observed.

6 Atmospheric implications and conclusions

The effect of aerosol viscosity upon HO_2 uptake coefficients was systematically investigated with a combination of HO_2 uptake coefficient measurements and a state-of-the-art kinetic model. A good correlation was obtained between measured HO_2 uptake coefficients onto copper-doped sucrose aerosols as a function of RH and the KM-SUB model output. At higher relative humidities the uptake was limited by mass accommodation, whilst at lower relative humidities the aerosol particles were viscous and the uptake was limited by surface reaction. These results imply that viscous aerosol particles will have very little impact upon gaseous tropospheric HO_2 concentrations.

The first measurements of the HO_2 uptake coefficient onto SOA have been reported in this work. The HO_2 uptake coefficient measured for α-pinene-derived aerosol particles was below the limit of detection of the apparatus ($\gamma < 0.001$), whereas for TMB-derived aerosol particles the uptake coefficient was measurable ($\gamma = 0.004 \pm 0.002$). These results are consistent with the copper-doped sucrose results, and indicate that the impact of SOA on gaseous HO_2 concentrations would likely be small. However, it remains unclear as to the reasons for the larger HO_2 uptake coefficient measured on TMB-derived aerosol particles compared to α-pinene-derived aerosol particles. The possibility that the larger uptake coefficient onto TMB-derived aerosol particles was due to a lower viscosity of the aerosol particles or a higher liquid water content compared to α-pinene-derived aerosol particles cannot be confirmed until further measurements of the viscosity and liquid water content of TMB-derived aerosol particles are published in the literature. However, if the larger uptake coefficients are due to an $HO_2 + RO_2$ reaction within the aerosol, this could impact the HO_2 uptake coefficient for any aerosol containing RO_2. The actual increase would depend on a variety of factors such as the concentrations of RO_2, the partition coefficients of RO_2 to the aerosol particles, the reactivity of different RO_2 species with HO_2 radicals, and the particle-phase formation of RO_2 and other reactive radicals (Lee et al., 2016; Donahue et al., 2012; Tong et al., 2016). The $HO_2 + RO_2$ reaction could potentially occur within the majority of aerosol particles within the atmosphere, this could have implications for the gaseous HO_2 and RO_2 concentrations in the troposphere which could then impact upon the concentrations of other species such as ozone.

Acknowledgements. Pascale S. J. Lakey is grateful to NERC for the award of a studentship. Lisa K. Whalley and Dwayne E. Heard are also grateful to the NERC funded National Centre for Atmospheric Science for ongoing support and to NERC for funding of the HO_2 aerosol uptake apparatus (grant reference NE/F020651/1). Thomas Berkemeier was supported by the Max Planck Graduate Center with the Johannes Gutenberg-Universität Mainz (MPGC). The experiments at PSI were supported by T. Bartels-Rausch and M. Birrer. Markus Ammann and Manuel Krapf were supported by the Swiss National Science Foundation (grant nos. 149492, CR3213-140851).

Edited by: F. Keutsch
Reviewed by: two anonymous referees

References

Ammann, M.: Using ^{13}N as tracer in heterogeneous atmospheric chemistry experiments, Radiochim. Acta, 89, 831–838, 2001.

Arens, F., Gutzwiller, L., Baltensperger, U., Gäggeler, H. W., and Ammann, M.: Heterogeneous reaction of NO_2 on diesel soot particles, Environ. Sci. Technol., 35, 2191–2199, 2001.

Badger, C. L., Griffiths, P. T., George, I., Abbatt, J. P. D., and Cox, R. A.: Reactive uptake of N_2O_5 by aerosol particles containing mixtures of humic acid and ammonium sulfate, J. Phys. Chem. A, 110, 6986–6994, doi:10.1021/jp0562678, 2006.

Bedjanian, Y., Romanias, M. N., and El Zein, A.: Uptake of HO_2 radicals on Arizona Test Dust, Atmos. Chem. Phys., 13, 6461–6471, doi:10.5194/acp-13-6461-2013, 2013.

Behr, P., Scharfenort, U., Ataya, K., and Zellner, R.: Dynamics and mass accommodation of HCl molecules on sulfuric acid–water surfaces, Phys. Chem. Chem. Phys., 11, 8048–8055, 2009.

Berkemeier, T., Huisman, A. J., Ammann, M., Shiraiwa, M., Koop, T., and Pöschl, U.: Kinetic regimes and limiting cases of gas uptake and heterogeneous reactions in atmospheric aerosols and clouds: a general classification scheme, Atmos. Chem. Phys., 13, 6663–6686, doi:10.5194/acp-13-6663-2013, 2013.

Berkemeier, T., Shiraiwa, M., Pöschl, U., and Koop, T.: Competition between water uptake and ice nucleation by glassy organic aerosol particles, Atmos. Chem. Phys., 14, 12513–12531, doi:10.5194/acp-14-12513-2014, 2014.

Berkemeier, T., Steimer, S. S., Krieger, U. K., Peter, T., Pöschl, U., Ammann, M., and Shiraiwa, M.: Ozone uptake on glassy, semi-solid and liquid organic matter and the role of reactive oxygen intermediates in atmospheric aerosol chemistry, Phys. Chem. Chem. Phys., 18, 12662–12674, 2016.

Bones, D. L., Reid, J. P., Lienhard, D. M., and Krieger, U. K.: Comparing the mechanism of water condensation and evaporation in glassy aerosol, P. Natl. Acad. Sci. USA, 109, 11613–11618, doi:10.1073/pnas.1200691109, 2012.

Brown, R. L.: Tubular Flow Reactors With 1st-Order Kinetics, J. Res. Nat. Bur. Stand., 83, 1–8, 1978.

Bruns, E. A., El Haddad, I., Keller, A., Klein, F., Kumar, N. K., Pieber, S. M., Corbin, J. C., Slowik, J. G., Brune, W. H., Baltensperger, U., and Prévôt, A. S. H.: Inter-comparison of laboratory smog chamber and flow reactor systems on organic aerosol yield and composition, Atmos. Meas. Tech., 8, 2315–2332, doi:10.5194/amt-8-2315-2015, 2015.

Calvert, J. G., Atkinson, R., Becker, K. H., Kamens, R. M., Seinfeld, J. H., Wallington, T. J., and Yarwood, G.: The Mechanisms of Atmospheric Oxidation of Aromatic Hydrocarbons, Oxford University Press, Oxford, 2002.

Champion, D., Hervet, H., Blond, G., Le Meste, M., and Simatos, D.: Translational diffusion in sucrose solutions in the vicinity of their glass transition temperature, J. Phys. Chem. B, 101, 10674–10679, 1997.

Davidovits, P., Kolb, C. E., Williams, L. R., Jayne, J. T., and Worsnop, D. R.: Mass accommodation and chemical reactions at gas-liquid interfaces, Chem. Rev., 106, 1323–1354, doi:10.1021/cr040366k, 2006.

Davies, J. F. and Wilson, K. R.: Nanoscale interfacial gradients formed by the reactive uptake of OH radicals onto viscous aerosol surfaces, Chem. Sci., 6, 7020–7027, 2015.

Donahue, N. M., Henry, K. M., Mentel, T. F., Kiendler-Scharr, A., Spindler, C., Bohn, B., Brauers, T., Dorn, H. P., Fuchs, H., and Tillmann, R.: Aging of biogenic secondary organic aerosol via gas-phase OH radical reactions, P. Natl. Acad. Sci. USA, 109, 13503–13508, 2012.

Duplissy, J., DeCarlo, P. F., Dommen, J., Alfarra, M. R., Metzger, A., Barmpadimos, I., Prevot, A. S. H., Weingartner, E., Tritscher, T., Gysel, M., Aiken, A. C., Jimenez, J. L., Canagaratna, M. R., Worsnop, D. R., Collins, D. R., Tomlinson, J., and Baltensperger, U.: Relating hygroscopicity and composition of organic aerosol particulate matter, Atmos. Chem. Phys., 11, 1155–1165, doi:10.5194/acp-11-1155-2011, 2011.

Fowler, D., Pilegaard, K., Sutton, M., Ambus, P., Raivonen, M., Duyzer, J., Simpson, D., Fagerli, H., Fuzzi, S., and Schjørring, J. K.: Atmospheric composition change: ecosystems–atmosphere interactions, Atmos. Environ., 43, 5193–5267, 2009.

Fuchs, H., Bohn, B., Hofzumahaus, A., Holland, F., Lu, K. D., Nehr, S., Rohrer, F., and Wahner, A.: Detection of HO_2 by laser-induced fluorescence: calibration and interferences from RO_2 radicals, Atmos. Meas. Tech., 4, 1209–1225, doi:10.5194/amt-4-1209-2011, 2011.

Fuchs, N. A. and Sutugin, A. G.: Properties of Highly Dispersed Aerosols, Ann Arbor Science Publishers, Ann Arbor, Michigan, 1970.

George, I. J., Matthews, P. S. J., Whalley, L. K., Brooks, B., Goddard, A., Baeza-Romero, M. T., and Heard, D. E.: Measurements of uptake coefficients for heterogeneous loss of HO_2 onto submicron inorganic salt aerosols, Phys. Chem. Chem. Phys., 15, 12829–12845, doi:10.1039/C3CP51831K, 2013.

Gržinić, G., Bartels-Rausch, T., Berkemeier, T., Türler, A., and Ammann, M.: Viscosity controls humidity dependence of N_2O_5 uptake to citric acid aerosol, Atmos. Chem. Phys., 15, 13615–13625, doi:10.5194/acp-15-13615-2015, 2015.

Hanson, D. R., Ravishankara, A., and Solomon, S.: Heterogeneous reactions in sulfuric acid aerosols: A framework for model calculations, J. Geophys. Res.-Atmos., 99, 3615–3629, 1994.

Heard, D. E. and Pilling, M. J.: Measurement of OH and HO_2 in the troposphere, Chem. Rev., 103, 5163–5198, doi:10.1021/cr020522s, 2003.

Houle, F., Hinsberg, W., and Wilson, K.: Oxidation of a model alkane aerosol by OH radical: the emergent nature of reactive uptake, Phys. Chem. Chem. Phys., 17, 4412–4423, 2015.

Jacob, D. J.: Heterogeneous chemistry and tropospheric ozone, Atmos. Environ., 34, 2131–2159, 2000.

Kanakidou, M., Seinfeld, J. H., Pandis, S. N., Barnes, I., Dentener, F. J., Facchini, M. C., Van Dingenen, R., Ervens, B., Nenes, A., Nielsen, C. J., Swietlicki, E., Putaud, J. P., Balkanski, Y., Fuzzi, S., Horth, J., Moortgat, G. K., Winterhalter, R., Myhre, C. E. L., Tsigaridis, K., Vignati, E., Stephanou, E. G., and Wilson, J.: Organic aerosol and global climate modelling: a review, Atmos. Chem. Phys., 5, 1053–1123, doi:10.5194/acp-5-1053-2005, 2005.

Kanaya, Y., Cao, R., Kato, S., Miyakawa, Y., Kajii, Y., Tanimoto, H., Yokouchi, Y., Mochida, M., Kawamura, K., and Akimoto, H.: Chemistry of OH and HO_2 radicals observed at Rishiri Island, Japan, in September 2003: Missing daytime sink of HO_2 and positive nighttime correlations with monoterpenes, J. Geophys. Res.-Atmos., 112, D11308, doi:10.1029/2006jd007987, 2007.

Kang, E., Root, M. J., Toohey, D. W., and Brune, W. H.: Introducing the concept of Potential Aerosol Mass (PAM), Atmos. Chem. Phys., 7, 5727–5744, doi:10.5194/acp-7-5727-2007, 2007.

Lakey, P. S. J., George, I. J., Whalley, L. K., Baeza-Romero, M. T., and Heard, D. E.: Measurements of the HO_2 Uptake Coefficients onto Single Component Organic Aerosols, Environ. Sci. Technol., 49, 4878–4885, doi:10.1021/acs.est.5b00948, 2015a.

Lakey, P. S. J., George, I. J., Baeza-Romero, M. T., Whalley, L. K., and Heard, D. E.: Organics substantially reduce HO_2 uptake onto aerosols containing transition metal ions, J. Phys. Chem. A, 120, 1421–1430, 2015b.

Lambe, A. T., Ahern, A. T., Williams, L. R., Slowik, J. G., Wong, J. P. S., Abbatt, J. P. D., Brune, W. H., Ng, N. L., Wright, J. P., Croasdale, D. R., Worsnop, D. R., Davidovits, P., and Onasch, T. B.: Characterization of aerosol photooxidation flow reactors: heterogeneous oxidation, secondary organic aerosol formation and cloud condensation nuclei activity measurements, Atmos. Meas. Tech., 4, 445–461, doi:10.5194/amt-4-445-2011, 2011a.

Lambe, A. T., Onasch, T. B., Massoli, P., Croasdale, D. R., Wright, J. P., Ahern, A. T., Williams, L. R., Worsnop, D. R., Brune, W. H., and Davidovits, P.: Laboratory studies of the chemical composition and cloud condensation nuclei (CCN) activity of secondary organic aerosol (SOA) and oxidized primary organic aerosol (OPOA), Atmos. Chem. Phys., 11, 8913–8928, doi:10.5194/acp-11-8913-2011, 2011b.

Lee, B. H., Mohr, C., Lopez-Hilfiker, F. D., Lutz, A., Hallquist, M., Lee, L., Romer, P., Cohen, R. C., Iyer, S., and Kurtén, T.: Highly functionalized organic nitrates in the southeast United States: Contribution to secondary organic aerosol and reactive nitrogen budgets, P. Natl. Acad. Sci. USA, 113, 1516–1521, 2016.

Lienhard, D. M., Huisman, A. J., Krieger, U. K., Rudich, Y., Marcolli, C., Luo, B. P., Bones, D. L., Reid, J. P., Lambe, A. T., Canagaratna, M. R., Davidovits, P., Onasch, T. B., Worsnop, D. R., Steimer, S. S., Koop, T., and Peter, T.: Viscous organic aerosol particles in the upper troposphere: diffusivity-controlled water uptake and ice nucleation?, Atmos. Chem. Phys., 15, 13599–13613, doi:10.5194/acp-15-13599-2015, 2015.

Lim, H. J. and Turpin, B. J.: Origins of primary and secondary organic aerosol in Atlanta: Results' of time-resolved measurements during the Atlanta supersite experiment, Environ. Sci. Technol., 36, 4489–4496, doi:10.1021/es0206487, 2002.

Lu, J. W., Rickards, A. M., Walker, J. S., Knox, K. J., Miles, R. E., Reid, J. P., and Signorell, R.: Timescales of water transport in viscous aerosol: measurements on sub-micron particles and dependence on conditioning history, Phys. Chem. Chem. Phys., 16, 9819–9830, doi:10.1039/c3cp54233e, 2014.

Mao, J., Jacob, D. J., Evans, M. J., Olson, J. R., Ren, X., Brune, W. H., St Clair, J. M., Crounse, J. D., Spencer, K. M., Beaver, M. R., Wennberg, P. O., Cubison, M. J., Jimenez, J. L., Fried, A., Weibring, P., Walega, J. G., Hall, S. R., Weinheimer, A. J., Cohen, R. C., Chen, G., Crawford, J. H., McNaughton, C., Clarke, A. D., Jaegle, L., Fisher, J. A., Yantosca, R. M., Le Sager, P., and Carouge, C.: Chemistry of hydrogen oxide radicals (HO_x) in the Arctic troposphere in spring, Atmos. Chem. Phys., 10, 5823–5838, doi:10.5194/acp-10-5823-2010, 2010.

Marshall, F. H., Miles, R. E., Song, Y.-C., Ohm, P. B., Power, R. M., Reid, J. P., and Dutcher, C. S.: Diffusion and reactivity in ultraviscous aerosol and the correlation with particle viscosity, Chem. Sci., 7, 1298–1308, 2016.

Matthews, P. S. J., Baeza-Romero, M. T., Whalley, L. K., and Heard, D. E.: Uptake of HO_2 radicals onto Arizona test dust particles using an aerosol flow tube, Atmos. Chem. Phys., 14, 7397–7408, doi:10.5194/acp-14-7397-2014, 2014.

Ortega, A. M., Hayes, P. L., Peng, Z., Palm, B. B., Hu, W., Day, D. A., Li, R., Cubison, M. J., Brune, W. H., Graus, M., Warneke, C., Gilman, J. B., Kuster, W. C., de Gouw, J., Gutiérrez-Montes, C., and Jimenez, J. L.: Real-time measurements of secondary organic aerosol formation and aging from ambient air in an oxidation flow reactor in the Los Angeles area, Atmos. Chem. Phys., 16, 7411–7433, doi:10.5194/acp-16-7411-2016, 2016.

Paulsen, D., Dommen, J., Kalberer, M., Prévôt, A. S. H., Richter, R., Sax, M., Steinbacher, M., Weingartner, E., and Baltensperger, U.: Secondary Organic Aerosol Formation by Irradiation of 1,3,5-Trimethylbenzene-NO_x-H_2O in a New Reaction Chamber for Atmospheric Chemistry and Physics, Environ. Sci. Technol., 39, 2668–2678, doi:10.1021/es0489137, 2005.

Pöschl, U. and Shiraiwa, M.: Multiphase Chemistry at the Atmosphere–Biosphere Interface Influencing Climate and Public Health in the Anthropocene, Chem. Rev., 115, 4440–4475, 2015.

Power, R., Simpson, S., Reid, J., and Hudson, A.: The transition from liquid to solid-like behaviour in ultrahigh viscosity aerosol particles, Chem. Sci., 4, 2597–2604, 2013.

Price, H. C., Murray, B. J., Mattsson, J., O'Sullivan, D., Wilson, T. W., Baustian, K. J., and Benning, L. G.: Quantifying water diffusion in high-viscosity and glassy aqueous solutions using a Raman isotope tracer method, Atmos. Chem. Phys., 14, 3817–3830, doi:10.5194/acp-14-3817-2014, 2014.

Qi, L., Nakao, S., and Cocker III, D. R.: Aging of secondary organic aerosol from α-pinene ozonolysis: Roles of hydroxyl and nitrate radicals, J. Air Waste Manage., 62, 1359–1369, 2012.

Renbaum-Wolff, L., Grayson, J. W., Bateman, A. P., Kuwata, M., Sellier, M., Murray, B. J., Shilling, J. E., Martin, S. T., and Bertram, A. K.: Viscosity of alpha-pinene secondary organic material and implications for particle growth and reactivity, P. Natl. Acad. Sci. USA, 110, 8014–8019, doi:10.1073/pnas.1219548110, 2013.

Sander, S. P., Friedl, R. R., Golden, D. M., Kurylo, M. J., Huie, R. E., Orkin, V. L., Moortgat, G. K., Ravishankara, A. R., Kolb, C. E., Molina, M. J., and Finlayson-Pitts, B. J.: Chemical Kinetics and Photochemical Data for Use in Atmospheric Studies, JPL Publications Publication no. 02-25, NASA, http://jpldataeval.jpl.nasa.gov/ (last access: October 2016), 2003.

Schwartz, S. and Freiberg, J.: Mass-transport limitation to the rate of reaction of gases in liquid droplets: Application to oxidation of SO_2 in aqueous solutions, Atmos. Environ., 15, 1129–1144, 1981.

Shiraiwa, M., Pfrang, C., and Pöschl, U.: Kinetic multi-layer model of aerosol surface and bulk chemistry (KM-SUB): the influence of interfacial transport and bulk diffusion on the oxidation of oleic acid by ozone, Atmos. Chem. Phys., 10, 3673–3691, doi:10.5194/acp-10-3673-2010, 2010.

Shiraiwa, M., Sosedova, Y., Rouvière, A., Yang, H., Zhang, Y., Abbatt, J. P., Ammann, M., and Pöschl, U.: The role of long-lived reactive oxygen intermediates in the reaction of ozone with aerosol particles, Nat. Chem., 3, 291–295, 2011a.

Shiraiwa, M., Ammann, M., Koop, T., and Pöschl, U.: Gas uptake and chemical aging of semisolid organic aerosol particles, P. Natl. Acad. Sci. USA, 108, 11003–11008, 2011b.

Slade, J. H. and Knopf, D. A.: Multiphase OH oxidation kinetics of organic aerosol: The role of particle phase state and relative humidity, Geophys. Res. Lett., 41, 5297–5306, 2014.

Steimer, S. S., Lampimäki, M., Coz, E., Grzinic, G., and Ammann, M.: The influence of physical state on shikimic acid ozonolysis: a case for in situ microspectroscopy, Atmos. Chem. Phys., 14, 10761–10772, doi:10.5194/acp-14-10761-2014, 2014.

Steimer, S. S., Berkemeier, T., Gilgen, A., Krieger, U. K., Peter, T., Shiraiwa, M., and Ammann, M.: Shikimic acid ozonolysis kinetics of the transition from liquid aqueous solution to highly viscous glass, Phys. Chem. Chem. Phys., 17, 31101–31109, 2015.

Stone, D., Whalley, L. K., and Heard, D. E.: Tropospheric OH and HO_2 radicals: field measurements and model comparisons, Chem. Soc. Rev., 41, 6348–6404, doi:10.1039/c2cs35140d, 2012.

Takahama, S. and Russell, L.: A molecular dynamics study of water mass accommodation on condensed phase water coated by fatty acid monolayers, J. Geophys. Res.-Atmos., 116, D02203, doi:10.1029/2010JD014842, 2011.

Taketani, F. and Kanaya, Y.: Kinetics of HO_2 Uptake in Levoglucosan and Polystyrene Latex Particles, J. Phys. Chem. Lett., 1, 1701–1704, doi:10.1021/jz100478s, 2010.

Taketani, F., Kanaya, Y., and Akimoto, H.: Kinetic Studies of Heterogeneous Reaction of HO_2 Radical by Dicarboxylic Acid Particles, Int. J. Chem. Kinet., 45, 560–565, doi:10.1002/kin.20783, 2013.

Thornton, J. A., Braban, C. F., and Abbatt, J. P. D.: N_2O_5 hydrolysis on sub-micron organic aerosols: the effect of relative humidity, particle phase, and particle size, Phys. Chem. Chem. Phys., 5, 4593–4603, doi:10.1039/B307498F, 2003.

Thornton, J. A., Jaegle, L., and McNeill, V. F.: Assessing known pathways for HO_2 loss in aqueous atmospheric aerosols: Regional and global impacts on tropospheric oxidants, J. Geophys. Res.-Atmos., 113, D05303, doi:10.1029/2007jd009236, 2008.

Tong, H., Arangio, A. M., Lakey, P. S. J., Berkemeier, T., Liu, F., Kampf, C. J., Brune, W. H., Pöschl, U., and Shiraiwa, M.: Hydroxyl radicals from secondary organic aerosol decomposition in water, Atmos. Chem. Phys., 16, 1761–1771, doi:10.5194/acp-16-1761-2016, 2016.

Vieceli, J., Roeselova, M., Potter, N., Dang, L. X., Garrett, B. C., and Tobias, D. J.: Molecular dynamics simulations of atmospheric oxidants at the air-water interface: Solvation and accommodation of OH and O_3, J. Phys. Chem. B, 109, 15876–15892, 2005.

Whalley, L. K., Furneaux, K. L., Goddard, A., Lee, J. D., Mahajan, A., Oetjen, H., Read, K. A., Kaaden, N., Carpenter, L. J., Lewis, A. C., Plane, J. M. C., Saltzman, E. S., Wiedensohler, A., and Heard, D. E.: The chemistry of OH and HO_2 radicals in the boundary layer over the tropical Atlantic Ocean, Atmos. Chem. Phys., 10, 1555–1576, doi:10.5194/acp-10-1555-2010, 2010.

Whalley, L. K., Blitz, M. A., Desservettaz, M., Seakins, P. W., and Heard, D. E.: Reporting the sensitivity of laser-induced fluorescence instruments used for HO_2 detection to an interference from RO_2 radicals and introducing a novel approach that enables HO_2 and certain RO_2 types to be selectively measured, Atmos. Meas. Tech., 6, 3425–3440, doi:10.5194/amt-6-3425-2013, 2013.

Zhou, S. M., Shiraiwa, M., McWhinney, R. D., Poschl, U., and Abbatt, J. P. D.: Kinetic limitations in gas-particle reactions arising from slow diffusion in secondary organic aerosol, Faraday Discuss., 165, 391–406, doi:10.1039/c3fd00030c, 2013.

Zobrist, B., Soonsin, V., Luo, B. P., Krieger, U. K., Marcolli, C., Peter, T., and Koop, T.: Ultra-slow water diffusion in aqueous sucrose glasses, Phys. Chem. Chem. Phys., 13, 3514–3526, doi:10.1039/c0cp01273d, 2011.